Eur. Phys. J. B **3**, 119–123 (1998)

THE EUROPEAN PHYSICAL JOURNAL B

Electrostatic surface shape resonances of a finite number of ridges

J.M. Pereira Jr., R.N. Costa Filho[a], V.N. Freire, and G.A. Farias

Departamento de Física, Universidade Federal do Ceará, Campus do Pici, Centro de Ciências Exatas, Caixa Postal 6030, 60455-760 Fortaleza, Ceará, Brazil

Received: 24 June 1997 / Received in final form: 5 September 1997 / Accepted: 15 September 1997

Abstract. The resonance properties of localized electrostatic surface modes associated with a finite number of ridges on an otherwise planar surface are investigated. Numerical solutions of the homogeneous integral equations that describe the electromagnetic fields in the vicinity of the ridges are used to obtain the dispersion relation of surface plasmons. The frequencies of the electrostatic surface shape resonances are calculated for ridges with Gaussian, Lorentzian, sinusoidal, exponential, and triangular profiles. We show the existence of splittings of the plasmon frequencies, which depends on the surface profile function and on the distance between the ridges. Considering the ridge with a sinusoidal profile, we obtain the limit on the number of ridges which generates a frequency splitting of the electrostatic surface shape resonances, whose frequency values converge to those of the dispersion relation of surface plasmons on one-dimensional sinusoidal grating.

PACS. 73.20.Mf Collective excitations (including plasmons and other charge-density excitations) – 78.66.Bz Metals and metallic alloys

1 Introduction

It is well known that Electrostatic and electromagnetic surface shape resonances (ESSR), *i.e.,* surface resonances that owe their existence to the geometric shape of the surface, has become an important research subject because their excitation on the surface of a dielectric medium leads to a strong enhancement of the electric field in the vicinity of the surface. They are solutions of Laplace's or Maxwell's equations, respectively, in the vicinity of a protuberance or indentation on an otherwise planar surface of dielectric medium embeded by vacuum. The increase of the Raman scattering cross section of molecules adsorbed on solid surfaces [1] and the enhancement of the second harmonic generation in the reflection of light from a metalic interface [2] are important physical processes closely related to ESSR. More recently, Sánchez-Gil [3] has studied the coupling of electromagnetic waves with metallic gratings of finite length.

Theoretical calculations have shown that the frequencies of ESSR modes are sensitive to the shape of the surface protuberance or indentation. In particular, the influence of single hemispherical [4], spherical [5], and spheroidal [6] profiles on ESSR modes was studied. Malshukov and Shekhmamet'ev [7] have calculated the first pair of ESSR frequencies of a plane surface with a single ridge defined by a Lorentzian profile function. Maradudin and Visscher [8] have considered protuberances with a general profile by employing the Rayleigh hypothesis, the Green's theorem, and the extinction theorem to obtain the homogenous integral equations satisfied by the Fourier transform of the electrostatic potentials. Following reference [8], Maradudin [9] was able to generalize the results of reference [7] for the one-dimensional Lorentzian profile, and also calculated the ESSR associated to protuberances of cylindrical symmetry about the normal of the surface. For an even one-dimensional profile, Maradudin [9] showed that the frequencies of the resonances were roughly symmetrically positioned around the frequency of surface plasmons on a plane surface, and suggested that a sinusoidal grating could be thought of as the result of a superposition of a periodic array of ridges on an otherwise planar surface. This implies that the frequencies of the surface resonances associated with each protuberance should broaden into bands as a consequence of the alignment.

All the previous ESSR calculations were done assuming the existence of *only* one protuberance or depression on an otherwise plane surface. This assumption might be valid for a corrugated surface if the ridges are not close enough to each other since the resonant fields are localized in the vicinity of each protuberance.

The aim of this work is to present ESSR calculations for a surface having one or more ridges, characterized by an even one-dimensional profile function. The results have been obtained by using the method which was developed by Maradudin and Visscher [8] to calculate ESSR

[a] e-mail: rai@fisica.ufc.fr

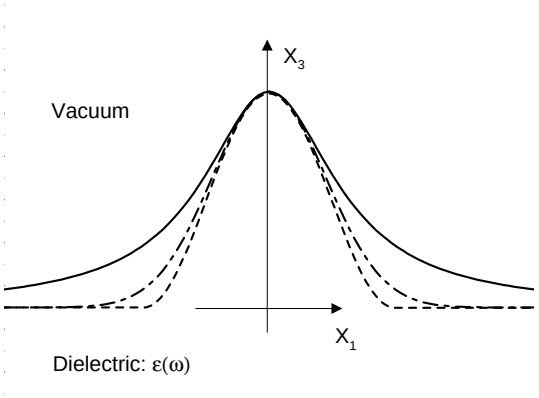

Fig. 1. Interface between vacuum and a half-space dielectric with an isolated ridge described by a Gaussian (dotted-dashed curve), Lorentzian (solid curve) and sinusoidal (dashed curve) profile.

frequencies in an otherwise planar surface of a semi-infinite medium with a real dielectric function of the free electron type.

2 Model

The system considered here consists of a half-space dielectric with vacuum above. The dielectric is characterized by an isotropic, real, frequency-dependent dielectric function $\epsilon(\omega)$ in the region $x_3 < \zeta(\mathbf{x}_\parallel)$, with $\mathbf{x}_\parallel = x_1\mathbf{e}_1 + x_2\mathbf{e}_2$, where $\mathbf{e}_1$ and $\mathbf{e}_2$ are unit vectors in the x and y directions, respectively. Figure 1 shows three different types of interfaces between the vacuum and the dielectric with one ridge, which will be discussed in this work. Since we do not include retardation effects, the resonance frequencies of the ESSR are determined by solving Laplace's equation. The electrostatic potential solutions of the Laplace equation outside the selvedge region $[\zeta(\mathbf{x}_\parallel)_{min} < x_3 < \zeta(\mathbf{x}_\parallel)_{max}]$ can be written in the form of Fourier integrals as:

$$\phi^{>}(\omega,\mathbf{x}) = \frac{1}{(2\pi)^2}\int a(\omega,\mathbf{k})\, e^{i\mathbf{k}.\mathbf{x}_\parallel - |\mathbf{k}|x_3}\, d^2\mathbf{k}, \quad x_3 > \zeta(\mathbf{x}_\parallel)_{max}, \tag{1a}$$

$$\phi^{<}(\omega,\mathbf{x}) = \frac{1}{(2\pi)^2}\int b(\omega,\mathbf{k})\, e^{i\mathbf{k}.\mathbf{x}_\parallel + |\mathbf{k}|x_3}\, d^2\mathbf{k}, \quad x_3 < \zeta(\mathbf{x}_\parallel)_{min}, \tag{1b}$$

where $\mathbf{k} = k_1\mathbf{e}_1 + k_2\mathbf{e}_2$, $\mathbf{x} = \mathbf{x}_\parallel + x_3\mathbf{e}_3$, and $a(\omega\mathbf{k})$ $[b(\omega,\mathbf{k})]$ is the Fourier coefficient of the electrostatic field in the vacuum [dielectric] respectively.

Taking into account the Rayleigh hypothesis [8], *i.e.* that the potentials given by equation (15) can be used inside the selvedge region, we obtain the boundary conditions given by

$$\phi^{>}(\omega,\mathbf{x})|_{x_3=\zeta(\mathbf{x}_\parallel)} = \phi^{<}(\omega,\mathbf{x})|_{x_3=\zeta(\mathbf{x}_\parallel)}, \tag{2a}$$

$$\frac{\partial\phi^{>}(\omega,\mathbf{x})}{\partial n}|_{x_3=\zeta(\mathbf{x}_\parallel)} = \epsilon(\omega)\frac{\partial\phi^{<}(\omega,\mathbf{x})}{\partial n}|_{x_3=\zeta(\mathbf{x}_\parallel)}. \tag{2b}$$

By using the method of Maradudin and Visscher [8] for a one-dimensional ridge described by an even profile function $\zeta(x_1)$, it can be straightforwardly shown that the coefficient $a(\omega,q)$ satisfies the homogeneous integral equation [9]

$$\lambda\, a(\omega,q) = \frac{1}{\pi}\int_0^\infty p\, a(\omega,p)\, J(q-p|q+p)\, dp, \tag{3}$$

with the kernel

$$J(q-p|q+p) = \int_{-\infty}^{\infty}\frac{e^{(q-p)\zeta(x_1)}-1}{q-p}\, e^{-i(q+p)x_1}\, dx_1, \tag{4a}$$

and

$$\lambda = \pm\,\frac{\epsilon(\omega)+1}{\epsilon(\omega)-1}\cdot \tag{4b}$$

The solvability condition of equation (3) yields the ESSR frequencies. Using a Gauss-Laguerre quadrature scheme [11]

$$\int_0^\infty dy\, e^{-y}\, f(y) = \sum_{j=1}^{N} w_j\, f(y_j), \tag{5}$$

where w_j (y_j) are the weights (abscissas), and N the number of abscissas, equation (3) can be converted into a matrix eigenvalue equation

$$\lambda\, a(\omega,\chi_i) = \sum_{j=1}^{N} M_{ij}\, a(\omega,\chi_j), \tag{6}$$

with

$$M_{ij} = \chi_j\, e^{\chi_j}\,\frac{4}{R^2}\, J(\chi_i-\chi_j|\chi_i+\chi_j)\, w_j, \tag{7}$$

and $q = 2\chi_i/R$, $p = 2\chi_j/R$, where R is the characteristic width of the profile function.

2.1 Single ridges

In order to study the influence of the profiles on the ESSR frequencies, we consider initially one isolated single ridge described by five different profiles. The first surface profile is defined by a Lorentzian function

$$\zeta(x_1) = \frac{A\,R^2/4}{x_1^2 + R^2/4}, \tag{8a}$$

where A represents the maximum height. In this case, the kernel $J(q-p|q+p)$ of the homogeneous integral is given by [9]

$$J(\xi-\chi|\xi+\chi) = \pi\,\frac{R}{4}^2\, e^{-2(\xi+\chi)} \times\sum_{n=1}^{\infty}\left(\frac{A}{R}\right)^n\frac{(\xi-\chi)}{n!}^{n-1}\, 2^n\,\frac{g_{n-1}[2(\xi+\chi)]}{(n-1)!}, \tag{8b}$$

where

$$g_{n+1}(z) = (2n+1)g_n(z) + z^2 g_{n-1}(z) \tag{9}$$

with $g_0(z) = 1$, $g_1(z) = z + 1$. The second profile is described by a Gaussian function

$$\zeta(x_1) = A e^{-4x_1^2/R^2}, \tag{10a}$$

and the corresponding kernel $J(q-p|q+p)$ is given by

$$J(\xi-\chi|\xi+\chi) = \frac{R^2}{4}\sqrt{\pi}\sum_{n=1}^{\infty}\left(\frac{A}{R}\right)^n \times \frac{(\xi-\chi)^{n-1}}{n!}\,\frac{2^n}{\sqrt{n}}\,\exp\left[-\frac{(\xi+\chi)^2}{4n}\right]. \tag{10b}$$

The third surface profile we consider is the following sinusoidal function

$$\zeta(x_1) = \begin{cases} 0 & x_1 < -L/2\,, \\ \frac{1}{2}\,A\,[1+\cos(\frac{2\pi}{L}x_1)] & -L/2 < x_1 < +L/2\,, \\ 0 & x_1 > +L/2\,, \end{cases} \tag{11a}$$

with A and L being the height and the period, respectively. In this case $J(q-p|q+p)$ is given by

$$J(\xi-\chi|\xi+\chi) = \frac{L^2}{4}\sum_{n=1}^{\infty}\left(\frac{A}{L}\right)^n \frac{(\xi-\chi)^{n-1}}{n!} \times \sum_{l=0}^{2n}(-1)^{n+l+1}\binom{2n}{l}\frac{\sin(\xi+\chi)}{[\pi(n-l)-(\xi+\chi)]}, \tag{11b}$$

with $\xi = Lq/2$ and $\chi = Lp/2$ in this case.

Although the Rayleigh hypothesis is valid only for analytic profiles [8,10], convergent results have been obtained with nonanalytic profiles. We have considered single ridges with profiles generated by functions whose first derivative is discontinuous. The first of these profiles is described by the following exponential function

$$\zeta(x_1) = A\,e^{-2|x_1|/R}, \tag{12a}$$

with the corresponding kernel given by

$$J(\xi-\chi|\xi+\chi) = R^2\sum_{n=1}^{\infty}\left(\frac{A}{R}\right)^n \times \frac{(\xi-\chi)^{n-1}}{n!}\,\frac{4}{n}\,\frac{1}{1+(\xi+\chi)/n^2}, \tag{12b}$$

with $\xi = R\,q$ and $\chi = R\,p$ in this case. The second nonanalytic profile is generated by a triangular function defined as

$$\zeta(x_1) = \begin{cases} 0, & x_1 < -R/2\,, \\ A(1-2|x_1|/R), & -R/2 < x_1 < +R/2\,, \\ 0, & x_1 > +R/2\,, \end{cases} \tag{13a}$$

which gives

$$J(\xi-\chi|\xi+\chi) = \frac{R^2}{4}\sum_{n=1}^{\infty}\left(\frac{A}{R}\right)^n \frac{(\xi-\chi)^{n-1}}{n!} \times 2^{n+1}\Big\{\sum_{l=0}^{n} l!\binom{n}{l}\left(\frac{1}{\xi+\chi}\right)^{l+1}\sin(\frac{l\pi}{2}) + n!\left(\frac{1}{\xi+\chi}\right)^{n+1}\sin(\xi+\chi-\frac{n\pi}{2})\Big\}. \tag{13b}$$

2.2 Multiple ridges

To analyse the behaviour of the ESSR frequencies when the surface of the dielectric has multiple ridges, we consider m ridges with a sinusoidal profile separated by a distance D. First, is considered a single sinusoidal ridge $\zeta_1(x_1)$ defined in an interval $-(L+D)/2 < x_1 < (L+D)/2$ as

$$\zeta_1(x_1) = \begin{cases} 0 & -(L+D)/2 < x_1 < -L/2 \\ \frac{1}{2}\,A\,[1+\cos(\frac{2\pi}{L}x_1)] & -L/2 < x_1 < L/2 \\ 0 & L/2 < x_1 < (L+D)/2 \end{cases}, \tag{14}$$

Consequently, the ensemble of m unidimensional sinusoidal ridges $\zeta_m(x_1)$ is described by

$$\zeta_m(x_1) = \begin{cases} 0, & -m(L+D)/2 < x_1 \\ \sum_{k=0}^{m-1}\zeta_1[x_1 + (m-2k-1)(1+\frac{D}{L})\frac{L}{2}]\,, & -m(L+D)/2 < x_1 < m(L+D)/2 \\ 0, & m(L+D)/2 < x_1 \end{cases}, \tag{15a}$$

where each sinusoidal ridge is located at a distance D apart from its neighbourhood. It can be shown that for such a profile, the corresponding kernel can be written as

$$J_m(\alpha|\beta) = U_{m-1}\{\cos[\,\beta\frac{L}{2}(1+D/L)\,]\}\,J_1(\alpha|\beta), \tag{15b}$$

where $\alpha = q-p$, $\beta = p+q$, $U_{m-1}\{\cos[\,\beta\frac{L}{2}(1+D/L)\,]\}$ is a second kind Chebyshev polynomial [11], and $J_1(\alpha|\beta)$ is given by equation (11b).

3 Numerical results

To obtain the ESSR frequencies for all the different profiles, one has to calculate the eigenvalues of equation (6). The degree of convergence depends on the surface profile, and also on the distance between the ridges in the case of multiple ridges. These calculations have been performed for a medium with free-electron-like dielectric function $\epsilon(\omega) = 1 - \omega_p^2/\omega^2$ where ω_p is the plasma frequency. As the first step, we calculated the ESSR associated with an isolated ridge. In solving the matrix equation, equation (6), it was found that the dimension N of the matrix M_{ij}, equation (7), which corresponds to the number of points

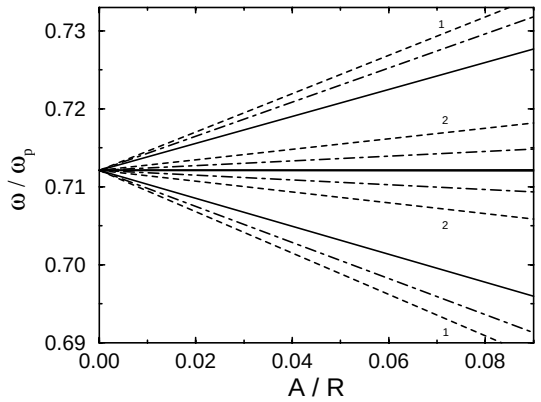

Fig. 2. The largest values of the resonance frequencies (1 and 2) of an isolated ridge as a function of the ratio A/R for a Gaussian (dotted-dashed curve), Lorentzian (solid curve) and sinusoidal (dashed curve) profile.

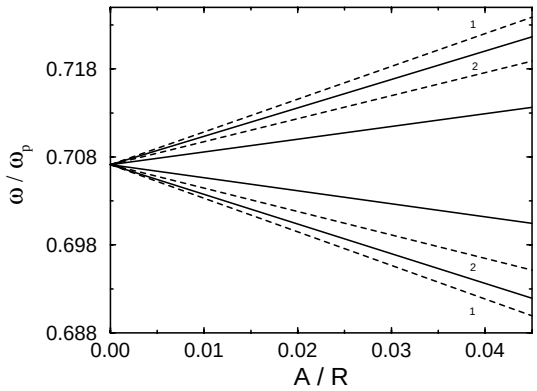

Fig. 3. The largest values of resonance frequencies (1 and 2) of an isolated ridge as a function of the ratio A/R for an exponential (solid curve) and triangular (dashed curve) profile.

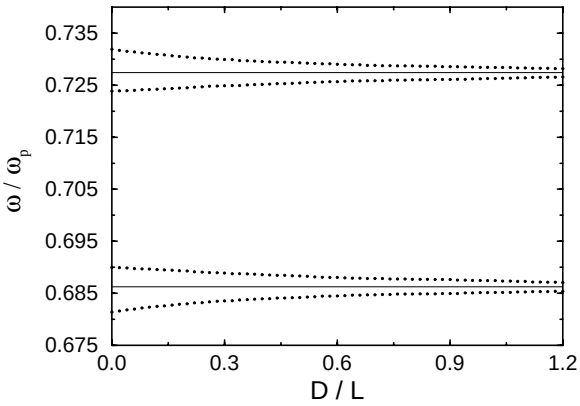

Fig. 4. The largest values of the resonance frequencies (dotted curve) for two ridges with a sinusoidal profile as a function of D/L, with $A/L = 0.05$. The solid curves represent the largest resonance frequencies of one single ridge.

used in the Gauss-Laguerre quadrature, depends on the surface profile through the ratio A/R (or A/L for the sinusoidal profile function), and on the number of terms n_j used in the summations of equations (8b, 10b, 11b, 12b, 13b, 15b) for each profile function. The Rayleigh hypothesis restricts the accuracy of the results to low values of A/R or A/L. In order to compare the resonance frequencies with the same ratio A/R for the first two profiles and A/L for the sinusoidal case, we consider the expansion of equations (8a, 10a, 11a) up to the second order, and take $R = 2L/\pi$ for the sinusoidal case. For the sinusoidal profile, we were able to achieve convergence for ratios A/L up to 0.15, which is of the same order as results obtained in previous calculations of the dispersion curves of surface waves propagating across sinusoidal gratings [9,12]. Due to the fact that there are two resonances for each value of λ, equation (4b), the method enables us to calculate a maximum of $2N$ frequencies.

Figure 2 shows the ESSR frequencies associated with the two largest values of $|\lambda|$ (1 and 2) for the Gaussian (dot-dashed curve), Lorentzian (solid curve) and sinusoidal (dashed curve) profiles as a function of the ratio A/R. A three figure accuracy was obtained for these resonance frequencies with $N = 5$ and $n_j = 2$, for ratios A/R or A/L up to 0.15. As can be seen, the frequencies are distributed roughly symmetrically with respect to $\omega_p/\sqrt{2}$. Considering the same ratio of A/R, the splitting depends strongly on the profile function, and the sinusoidal profile presents a larger splitting than the others. This is also observed for the second pair of resonance frequencies.

In Figure 3, we present the frequencies of the ESSR associated with the two largest values of $|\lambda|$ (1 and 2) for the exponential (solid curve) and triangular (dashed curve) profiles as a function to the ratio A/R. These profiles present a discontinuity in their first derivatives. The ESSR frequencies calculated with the triangular profile present a larger splitting than those calculated with the exponential profile. Despite the fact that these two profiles are described by nonanalytic functions, we were able to observe convergent solutions of equation (6) with three figure accuracy for values of A/R up to 0.07 and a 10 (15) quadrature for the exponential (triangular) profile. These limits are lower than those obtained with profiles whose first derivative is continuous, which is consistent with previous results obtained with the Rayleigh hypothesis for a grating surface [13].

In order to analyse the localization of the ESSR, we present in Figure 4 the largest resonance frequencies (dotted curve) for two ridges with a sinusoidal profile and $A/L = 0.05$, as a function of D/L. It is clear that these frequencies converge to the values obtained for a single ridge (solid curve) in a distance $D \approx L$, which implies that for this ratio of A/L, the ESSR are localized at this distance $D \approx L$, and consequently for distances larger than L the two ridges can be treated as isolated. Since the splitting between the frequencies increases with the ratio A/L, for larger values of this ratio, the distance on which two ridges can be treated as independent also increases. In order to observe the effects of multiple ridges, we consider $D = 0$ in equation (15a), and in Figure 5 we present the resonance frequencies for a sinusoidal profile with multiple ridges, $m = 1, 2, 3$, as a function of the ratio A/L. One can see that the number of branches increases

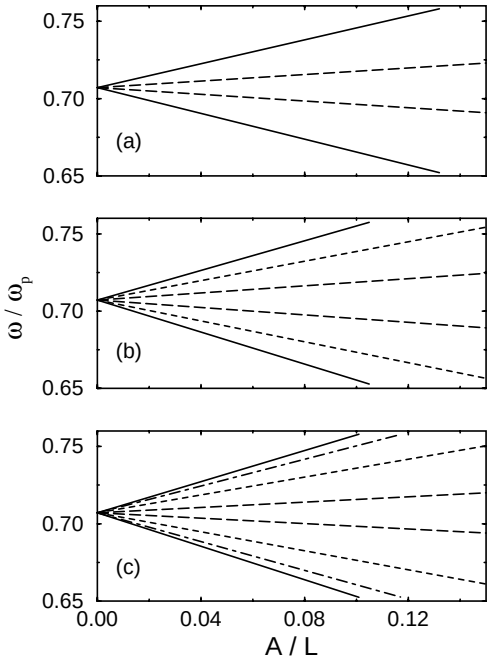

Fig. 5. Frequencies of the ESSR as functions of A/L for a sinusoidal profile with $D = 0$: (a) $m = 1$; (b) $m = 2$; and (c) $m = 3$.

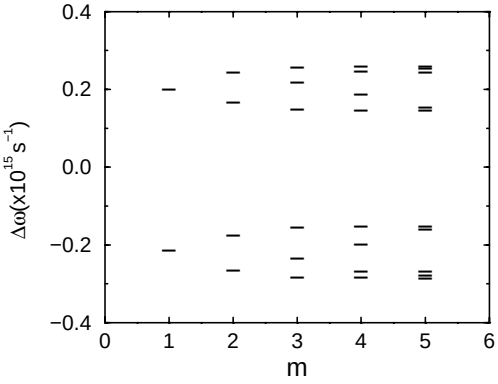

Fig. 6. Behaviour of the first pairs of resonance frequencies $\Delta\omega$ as a function of the number m of ridges when the dielectric medium is aluminum.

with m. Due to this fact, considering the same ratio A/L, the dimension of M_{ij}, equation (7), also increases with m in order to achieve good numerical accuracy. Particularly, for $A/L = 0.14$ we obtain three figure accuracy with $m = 1, 2, 3$, using $n_j = 2, 10, 25$, and matrices with dimensions $N = 5, 15$ and 20, respectively. The number of terms n_j must increase with N, which is due to the fact that the abscissae $\chi_{i,j}$ in equation (7) increase for larger values of N.

Considering aluminum as the surface active medium with a multiple sinusoidal profile, with $D = 0$ and $A/L = 0.14$, we show in Figure 6 the first pairs of resonance frequencies, $\Delta\omega = \omega - \omega_p/\sqrt{2}$ ($\omega_p = 3.699 \times 10^{15}$ s^{-1}), as a function of the number of ridges. As can be seen, when m increases the resonance frequencies present a larger number of branches. Also, the largest value of the splitting tends to the maximum value obtained by Glass and Maradudin [13], with the same ratio A/L, which indicates that for larger values of m one can assume the resonance frequencies to be those obtained for an infinite grating. In the case of $m = 5$, the results were obtained with three figure accuracy by using $N = 50$ and $n_j = 80$.

4 Conclusions

In conclusion, we have obtained the ESSR frequencies for one-dimensional ridges described by different profile functions. The splitting of the resonance frequencies depends strongly on the profile function. It has been shown that these ESSR modes are localized near the ridges, such that two ridges behave as isolated ones for relatively short distances. In grating surfaces, one of the previous works [13] has mentioned that it was difficult to observe experimentally the splitting of frequencies close to the frequency of the surface plasmons on a plane surface ($\omega_p/\sqrt{2}$). In the present case, the splitting on these frequencies depends strongly on the profile function, *e.g.*, the second pair of frequencies can be located far apart from the plasma frequency, allowing an easier experimental measurement. The number of branches increases with the number of ridges and, for a sinusoidal profile taking $m = 5$, the largest frequencies converge to those values obtained for a grating surface at the edge of the Brillouin zone . This indicates that the properties of a one-dimensional grating can be achieved with a relatively small number of ridges. The ESSR in other systems such as a film show a significative difference and are now under investigation.

This work was supported by the Brazilian National Research Council (CNPq).

References

1. *Surface Enhanced Raman Scattering*, edited by R.K. Chang, T.E. Furtak (Plenum, New York, 1982).
2. C.K. Chen, A.R.B. de Castro, Y.R. Shen, Phys. Rev. Lett. **46**, 145 (1981).
3. J.A. Sánches-Gil, Phys. Rev. B **53**, 10317 (1996), and references therein.
4. D.W. Berreman, Phys. Rev. **163**, 855 (1967).
5. R.W. Rendell, D.J. Scalapino, Phys. Rev. B **24**, 3276 (1978).
6. P.C. Das, J.L. Gersten, Phys. Rev. B **25**, 6281 (1982).
7. A.G. Mal'shukov, Sh. A. Shekhmamet'ev, Sov. Phys. - Solid State **25**, 1509 (1983).
8. A.A. Maradudin, W.M. Visscher, Z. Phys. B - Cond. Matter **60**, 215 (1985).
9. A.A. Maradudin, in *Electromagnetic Surface Excitations*, edited by R.F. Wallis, G.I. Stegeman (Springer-Verlag, 1986), p. 83.
10. R.F. Millar, Proc. Camb. Philos. Soc. **65**, 773 (1969).
11. M. Abramowitz, I.A. Stegun, *Handbook of Mathematical Functions*, (Dover, 1965).
12. A.A. Maradudin, in *Surface Polaritons*, edited by V.M. Agranovich, D.L. Mills (North-Holland, 1982), p. 453 .
13. N.E. Glass, A.A. Maradudin, Phys. Rev. B **24**, 595 (1981).